Earth and Planetary Science Letters 569 (2021) 117046

Contents lists available at ScienceDirect

Earth and Planetary Science Letters

www.elsevier.com/locate/epsl

Timing of lunar Mg-suite magmatism constrained by SIMS U-Pb dating of Apollo norite 78238

Bidong Zhang [a,b,*], Yangting Lin [c], Desmond E. Moser [a], Paul H. Warren [b], Jialong Hao [c], Ivan R. Barker [a], Sean R. Shieh [a], Audrey Bouvier [d,a]

[a] The University of Western Ontario, Department of Earth Sciences, London, Ontario N6A 3K7, Canada
[b] Department of Earth, Planetary, and Space Sciences, University of California, Los Angeles, CA 90095, USA
[c] Key Laboratory of Earth and Planetary Physics, Institute of Geology and Geophysics, Chinese Academy of Sciences, Beijing 100029, China
[d] Universität Bayreuth, Bayerisches Geoinstitut, Bayreuth 95447, Germany

ARTICLE INFO

Article history:
Received 19 October 2020
Received in revised form 2 June 2021
Accepted 5 June 2021
Available online 30 June 2021
Editor: W.B. McKinnon

Keywords:
U-Pb
Mg-suite
SIMS
baddeleyite
zircon
lunar magma ocean

ABSTRACT

The lunar Mg-suite magmatic rocks are commonly thought to represent mafic intrusions into the anorthositic flotation crust of the lunar magma ocean (LMO). Their geochronology is, therefore, important for constraining evolution models of the LMO. Petrogenetic models of the Mg-suite hold that their parent magmas were derived from primary LMO sources (Mg-cumulates, An-rich plagioclase, and melts enriched in KREEP—potassium, rare earth elements, and phosphorus). Previous radiogenic isotopic age interpretations of Mg-suite and putatively older, related ferroan anorthosites (FANs) overlap over a 200-million-year interval. The Apollo 78238 norite is an exemplary Mg-suite rock, with a relict coarse igneous texture modified by shock metamorphism. *In-situ* secondary ion mass spectrometry U-Pb analyses of zircon and baddeleyite in 78238 yield discordant arrays, attributed to recent impact metamorphism, with upper intercepts that constrain its crystallization age. The four oldest baddeleyite analyses give a weighted mean $^{207}Pb/^{206}Pb$ age of 4332 ± 18 Ma (2σ, MSWD = 0.06, P = 0.98), which is interpreted as the crystallization age of the norite. The overlap of the baddeleyite age with previously reported Sm-Nd and Pb-Pb mineral isochron ages for 78238 (Edmunson et al., 2009) supports a moderately fast cooling of the norite. Moreover, it is distinguishably younger than the most precisely dated sample of FAN (Apollo 60025), measured at 4360 ± 3 Ma by Sm-Nd and Pb-Pb mineral isochrons (Borg et al., 2011). Together with the baddeleyite $^{207}Pb/^{206}Pb$ age of Apollo Mg-suite troctolite 76535 at 4328 ± 8 Ma (White et al., 2020), the chronological record of the 78238 norite indicates a significant Mg-suite magmatic event at 4.33 Ga and a lower age limit on LMO differentiation.

1. Introduction

According to the lunar magma ocean (LMO) model, crystallization-differentiation influenced by gravity took place with dense silicates (olivine and orthopyroxene) descending to create an ultramafic mantle and buoyant plagioclase ascending to form a ferroan anorthosite (FAN) crust during the late stage (Fig. 1A) (Warren, 1985). Ilmenite-bearing cumulates capped the mantle after major LMO differentiation (Elardo et al., 2011). The last residual liquid of the magma ocean was urKREEP, which is enriched in highly incompatible elements potassium (K), rare earth elements (REE), and phosphorus (P) (Warren and Wasson, 1979).

After the primordial LMO differentiation, the ilmenite-bearing cumulates and their underlying deep-mantle cumulates (olivine and orthopyroxene) were transposed due to gravitational instability (Elkins-Tanton et al., 2002), and this process is called the mantle overturn (Fig. 1C). During this mantle overturn, the upwelling ultramafic cumulates exceeded their solidus owing to adiabatic decompression, and the melts produced from the decompression hybridized the FANs and KREEP-rich lithologies at temperatures below 1300 °C (Shearer et al., 2015). These decompression and hybridization processes generated the parental magmas of the Mg-suite, which contains calcic plagioclase (An_{98-84}) and Mg-rich (molar [Mg/(Mg+Fe)] = 95–60) minerals (Shearer et al., 2015). The intrusion of remelted mantle cumulates into the lunar crust, with a tendency for assimilative interaction with urKREEP, resulted in elevated REE contents in the Mg-suite parental magmas (Shearer et al., 2015). The fractional crystallization of such magmas might have produced a sequence of mineralogically continuous dunites,

* Corresponding author at: Department of Earth, Planetary, and Space Sciences, University of California, Los Angeles, CA 90095, USA.
E-mail address: bdzhang@ucla.edu (B. Zhang).

https://doi.org/10.1016/j.epsl.2021.117046

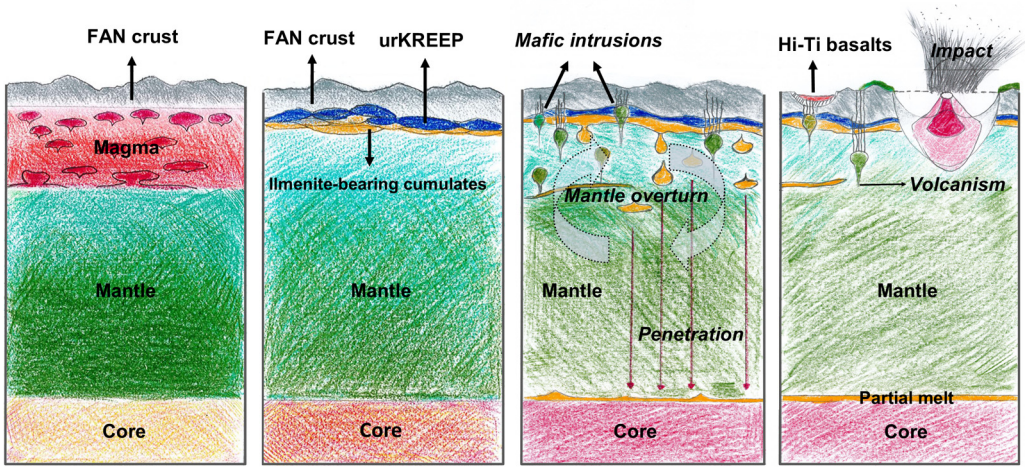

Fig. 1. Schematic of the early evolution of the lunar interior. **A**: Mafic components sink to form the mantle, and the segregation of buoyant FANs; **B**: The primordial LMO differentiates upon cooling (mafic cumulates, FANs, and urKREEP reservoir); **C**: After primordial differentiation, dense ilmenite-bearing cumulates are transposed and inversed with the overlying mafic cumulates, triggering the so-called lunar mantle overturn. Some Ti-rich melts remain in the mantle due to buoyancy, while denser melts penetrate the mantle and reach the mantle-core boundary. The volatile-rich ilmenite-bearing cumulates form a partial melt layer between the lunar mantle and core. Mafic melts ascend and intrude the crust. These intrusions are likely the source of the Mg-suite parental magmas. **D**: Subsequent volcanism and impacts modify the morphology of the Moon. The schematic size of each object or unit may not be scaled to its actual size.

troctolites, norites, and gabbronorites, and later the alkali-suite lithologies (Shearer et al., 2015). Another origin proposed for the Mg-suite is by impact melt sheet formation. This hypothesis holds that early impacts (at ~4.3 Ga) with the hot crust promoted the mixing of FANs and mantle materials (probably also urKREEP liquids) to form the Mg-suite parental magmas, which then intruded the crust (Hess, 1994; Shearer et al., 2015).

Regardless of the petrogenesis of the Mg-suite, as a post-LMO product, it serves as an important lower limit for the timeline of LMO differentiation. Radiogenic isotopic ages for the Mg-suite have added valuable constraints to the LMO model. The average Sm-Nd model ages of equilibration of the mare basalt source (i.e., much of the lunar mantle) at 4333 ± 30 Ma and urKREEP formation at 4350 ± 34 Ma suggest that the last stage of LMO differentiation might have taken only a few tens of million years (Borg et al., 2020 and references therein). The short duration of the last stage is further supported by the most precisely measured FAN age of Apollo 60025 at 4360 ± 3 Ma by Pb-Pb and ^{147}Sm–^{143}Nd isochrons (Borg et al., 2011) and by lunar zircon ^{207}Pb/^{206}Pb ages clustering at ~4340 Ma (e.g., Borg et al., 2015 and references therein; Crow et al., 2016; Grange et al., 2009; Nemchin et al., 2008). The Sm-Nd isochron age of collective Apollo Mg-suite rocks at 4348 ± 25 Ma (Borg et al., 2020) constrains that the LMO was differentiated before then and that the mantle overturn process might have been completed immediately after the LMO differentiation. The overlapping ages of these differentiated suites from radiogenic isotope chronometers (Sm-Nd, Lu-Hf, and U-Pb) with different closure temperatures also suggests cooling within a relatively short period of 30 Myr. The overlapping ages of the lunar differentiated suites are notable because the earliest-crystallized FANs should predate the post-LMO Mg-suite according to the LMO model, whereas the isochron ages of these two suites have not been resolved with current dating precision (Borg et al., 2015, 2020).

For the FANs and Mg-suite, radiometric internal mineral/whole rock isochron dating is the most common method used for obtaining their crystallization ages. The internal mineral/whole-rock isochrons have previously been obtained from rock-forming igneous minerals (pyroxene and feldspar) and whole rocks for systems based on long-lived radiogenic pairs such as ^{87}Rb-^{87}Sr, ^{147}Sm-^{143}Nd, ^{238,235}U-^{206,207}Pb, or ^{176}Lu-^{176}Hf (e.g., Borg et al., 2011, 2020; Carlson et al., 2014; Edmunson et al., 2009; Nyquist et al., 1981; Premo and Tatsumoto, 1991). Isochron ages can vary in precision owing to the generally limited fractionation of the parent/daughter elements between igneous minerals. Additionally, virtually all lunar FANs and Mg-suite rocks have a history of shock metamorphism, which may in some cases result in scattered points on the isochron diagrams and varying ages in different pieces of a sample analyzed in different laboratories (see section 2.1 for Apollo 76535 and 78238 as examples). Lunar Sm-Nd and Lu-Hf systematics can be affected by the neutron capture effects due to long-term exposure to cosmic rays and have to be appropriately corrected (Sprung et al., 2013). The U-Pb systematics can be disturbed by shock metamorphism due to the volatility of Pb and by sample handling processes (Edmunson et al., 2009). Therefore, determining precise and accurate isochron ages for the FANs and Mg-suite rocks is challenging.

Individual U-rich accessory minerals, such as zircon and baddeleyite, are excellent candidates to provide more precise and accurate ion-microprobe U-Pb and Pb-Pb dating of lunar samples owing to the generally high U content, low initial common Pb, and absence of neutron capture correction (e.g., Nemchin et al., 2009). Lunar zircons have been extensively used to constrain the differentiation of the lunar interior. They are associated with magmas that are enriched in incompatible elements and, thus, crystallized most abundantly from KREEP-rich melts. With the methodologic development of high-spatial-resolution U-Pb dating by secondary ion mass spectrometry (SIMS) with correlative microscopy techniques (e.g., White et al., 2020; Zhang et al., 2019, 2021), small U-rich minerals in less KREEPy highland rocks can be used to distinguish crystallization and metamorphic U-Pb ages with higher confidence. A recent *in-situ* Pb-Pb dating by SIMS of a baddeleyite grain from Apollo troctolite 76535 has been reported to have an age of 4328 ± 8 Ma (White et al., 2020). This age is the most precise age so far obtained for a Mg-suite rock.

Apollo 17 Station 8 norite boulder (samples 78235, 78236, 78238) is one of the most pristine (in terms of petrologic texture and highly siderophile element abundance) Mg-suite rocks (Warren, 1993). The boulder has been dated by multiple radiometric systematics. To date, the most accurately and precisely dated mineral isochron ages for the boulder are 4333 ± 59 Ma by Pb-Pb and 4334 ± 37 Ma by Sm-Nd (Edmunson et al., 2009). These ages with relatively large errors overlap with the age of FAN 60025 of 4360 ± 3 Ma (Borg et al., 2011). In this study, we performed microstructural microscopy analyses and *in-situ* NanoSIMS U-Pb and

Pb-Pb dating of zircon and baddeleyite grains from 78238 to obtain a more detailed chronology of this norite. The dating results provide more precise constraints on the timing of Mg-suite magmatism and serve to clarify the temporal relationship between the Mg-suite and FANs.

2. Material and methods

2.1. Sample description

During the Apollo 17 mission, 78238 was sampled, together with 78235 and 78236, from a norite boulder at Station 8 (Fig. 2), the foot of the Sculptured Hills in the Taurus-Littrow valley. These three samples have identical mineralogy and petrology (Nyquist et al., 1981) and have thus been regarded as equivalent in petrogenesis and geochronology. The norite boulder is coated with shock-produced glass and is cross-cut by glass veins (Schmitt et al., 2017). It exhibits a folded, planar lamination, interpreted as a relict igneous cumulate texture, which suggests that it was excavated from the deep crust by a major impact event (Jackson et al., 1975). This speculation was later confirmed by textural analyses of the orthopyroxene (Takeda et al., 1982) and geochronologic data of sample 78236 (Nyquist et al., 1981). The boulder may have been excavated by small craters within the valley, but more likely was spalled off a noritic knob on the Sculptured Hills (Schmitt et al., 2017). The boulder has an exposure age of 262 ± 5 Ma determined by ^{38}Ar-^{37}Ar (Fernandes et al., 2013).

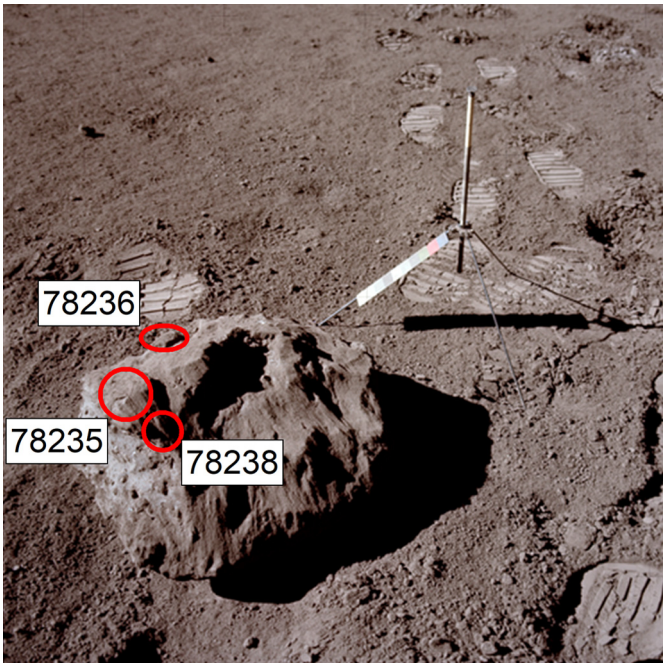

Fig. 2. A photograph (NASA AS17-146-22369) of the Station 8 norite. Samples 78235/6/8 (red circles) were chipped off from this boulder (Wolfe, 1974).

The boulder sub-samples Apollo 78235/6/8 also show this cumulate texture defined by coarse-grained plagioclase and orthopyroxene and no admixture of foreign materials (McCallum and Mathez, 1975). The samples have been described in the Lunar Compendium as approximately 40% plagioclase (0.3–1.0 cm, now maskelynite) and 60% orthopyroxene (0.2–0.7 cm) (Meyer, 2005). These two phases are bronzite ($En_{78}Wo_{19}Fs_3$) and anorthite (An_{97-93}) (Meyer, 2005). The accessory minerals include quartz, baddeleyite, chromite, clinopyroxene, apatite, and rutile (McCallum and Mathez, 1975). The shock effects in the plagioclase and pyroxene denote a shock pressure of 40–45 GPa and a post-shock temperature of 800–900 °C (Černok et al., 2019). After the impact, the norite re-equilibrated at 800 °C based on the partition of Fe and Mg between plagioclase and pyroxene (McCallum and Mathez, 1975). In spite of the intense shock effects, no recrystallization of the primary phases was identified (Takeda et al., 1982).

The Station 8 norite has been dated by multiple radiogenic isotopic systems (Fig. 3). The oldest crystallization age is 4430 ± 50 Ma by the ^{147}Sm-^{143}Nd method (Nyquist et al., 1981). A thermochronology age was determined by ^{40}Ar/^{39}Ar dating of the whole rock to be 4188 ± 26 Ma (Fernandes et al., 2013) and interpreted to represent a thermal disturbance event. The norite might have been subjected to an earlier impact event at 4270 ± 20 Ma according to the Ar-Ar age of its maskelynite separates (Fernandes et al., 2013; Nyquist et al., 1981), and this age has been taken as the lower age limit for the norite crystallization (Nyquist et al., 1981). Another two intermediate crystallization ages were derived from Sm-Nd systematics at 4320 ± 87 Ma (Nyquist et al., 2008) and 4340 ± 40 Ma (Carlson and Lugmair, 1981), respectively. More recent dating confirmed the ~4.3 Ga formation with concordant ages at 4334 ± 37 Ma, 4366 ± 53 Ma, and 4333 ± 59 Ma from Sm-Nd, Rb-Sr, and Pb-Pb mineral and whole-rock isotopic analyses, respectively (Edmunson et al., 2009).

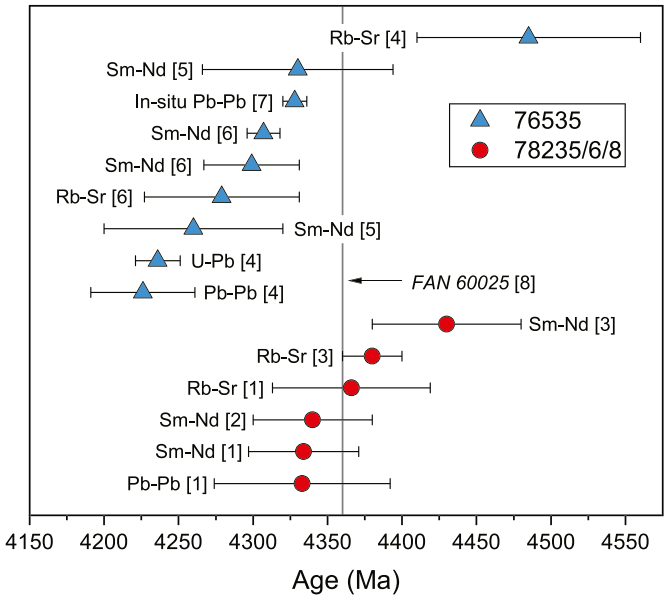

Fig. 3. Summary of Sm-Nd, U-Pb, Rb-Sr ages for the Apollo 78235/6/8 and 76535. These two samples are presented here as they are the most dated Mg-suite rocks using the mineral isochron methods. 76535 is presented here for comparison purposes, and its *in-situ* Pb-Pb age is from SIMS dating of a baddeleyite grain (White et al., 2020). All other ages shown on this diagram are derived from mineral isochron dating in the literature. References for 78235/6/8 ages correspond to [1] Edmunson et al. (2009), [2] Carlson and Lugmair (1981), and [3] Nyquist et al. (1981), and for 76535 correspond to [4] Premo and Tatsumoto (1992), [5] Lugmair et al. (1976), [6] Borg et al. (2017), [7] White et al. (2020). The age of FAN 60025 is from [8] Borg et al. (2011).

2.2. Cathodoluminescence (CL) and electron backscatter diffraction (EBSD)

We performed EBSD mapping and CL imaging of the only baddeleyite grain found in the 78238,14 thin section. Prior to mapping, the thin section was polished by neutral solution and colloidal 0.05-μm alumina polish for 20 min. The scanning electron microscopy (SEM) was performed with a Hitachi SU6600 VP-FEG SEM equipped with a Gatan Chroma CL detector and an Oxford Instruments Nordlys EBSD detector in the Zircon and Accessory Phase

Laboratory (ZAPLab) at The University of Western Ontario. The sample stage was tilted to 0° and 70° for CL and EBSD, respectively. The working distance was about 19 mm. The CL detector was operated by an accelerating voltage of 10 kV, and the EBSD detectors by a voltage of 20 kV. The electron backscatter diffraction patterns were collected at 55 ms/frame. To reduce the EBSP noise, we used an average frame of 4, binning of 4 × 4, and the high-gain mode. The EBSD mapping was performed by an Oxford HKL Channel 5 system.

2.3. U-Pb and trace-element abundance measurements

The U-Pb isotopes and selected trace elements (U, Th, and Y) were measured by the NanoSIMS 50L at the Institute of Geology and Geophysics, Chinese Academy of Sciences (IGGCAS). Prior to the NanoSIMS analyses, thin section 78238,14 was coated with carbon. Due to the small sizes of zircons in the thin section, for precise positioning of targeted grains under NanoSIMS, each grain was marked by two Pt bars (~10 μm) using a focused ion beam scanning electron microscopy (FIB-SEM) at IGGCAS. By doing so, the zircon and baddeleyite grains of interest can be relocated without sputtering much larger areas, and the small sputtering areas significantly improve the secondary ion yield. The NanoSIMS dating methods for zircon and baddeleyite are detailed in Yang et al. (2012) and Zhang et al. (2019). We used a 500-pA beam of $^{16}O^-$ that was optimized with L0 (5.6 kV) and L1 (5.1 kV). These settings allowed for the sensitivity of Pb^+ at ~4 cps/ppm/nA. The secondary ions were extracted using a co-axial immersion lens and passed to the mass spectrometer at a mass resolution of ~5000. The ^{204}Pb, ^{206}Pb, and ^{207}Pb isotopes were measured by the same electron multiplier using the magnetic peak-switching mode, and other species ($^{90}Zr_2^{16}O$, ^{238}U, $^{238}U^{16}O$, and $^{238}U^{16}O_2$) were measured by multiple electron multipliers simultaneously with ^{206}Pb using the same magnetic field. To remove the carbon coating and superficial contamination, sample surfaces were pre-sputtered for 3 min on an area of 20 × 20 μm^2. The primary rastering beam was 5 μm, and the analysis lasted for 30 min for each spot. The U-Pb ratios were corrected using the power-law relationship between $^{206}Pb/^{238}U$–$^{238}U^{16}O_2/^{238}U$ of reference zircon M257 (U-Pb age of 561 Ma) and of reference baddeleyite Phalaborwa (U-Pb age of 2059 Ma). The U, Th, and Y concentrations of zircon and baddeleyite were calculated using U/Zr, Th/Zr, and Y/Zr ratios, respectively, normalized to those of M257. For most lunar samples, U-rich minerals usually have low $^{204}Pb/^{206}Pb$ ratios ($<10^{-4}$), and the ^{204}Pb is primarily from superficial contamination during thin section polishing processes (Nemchin et al., 2008). The minor common Pb contribution of all zircon and baddeleyite analyses in this study was corrected using the modern Pb isotope composition from the Stacey-Kramer Pb growth model (Stacey and Kramers, 1975).

3. Results

3.1. Petrology of thin section 78238,14

Thin section 78238,14 has equivalent proportions of cumulus plagioclase (now mostly maskelynite) and orthopyroxene, and its minor phases include silica, troilite, zircon, and baddeleyite (Fig. 4). The pyroxene exhibits prevalent irregular fracturing and strong mosaicism under cross-polarized light (Fig. S1B). Some plagioclase grains display planar deformation features (Fig. S1A). We did not find any flow structures or evidence of high-temperature recrystallization of the major phases. In the lower right corner of the 78238,14 BSE image (Fig. 4), the cumulus pyroxene has been fragmented into smaller grains (<200 μm) contained in the plagioclase.

Microstructures attributable to shock metamorphism can also be seen in the accessory phases, zircon and baddeleyite, along with primary features. Four fine-grained (5–10 μm) zircons are enclosed within a large pyroxene grain (Fig. 4). These anhedral zircons are clustered together within a 100 × 100 μm^2 region (Fig. 5C). A few show dark cores and bright rims in CL, possibly remnant igneous growth zoning, but the internal zoning shows submicron offsets, likely due to shock metamorphic fracturing. Concentric zoning is not discernible in the remaining anhedral zircons that could have disaggregated from an originally larger grain. An anhedral baddeleyite grain (50 × 80 μm^2) resides (along with pyroxene chadacrysts) in the maskelynite (Fig. 4). From the absence of silica surrounding the baddeleyite grain (Fig. 5A), we infer that it remained ZrO_2 since its initial formation and did not form by decomposition of a zircon precursor. It shows subdomains of concentric CL zoning with dark cores and bright rims offset by microfractures. Measurement of microstructure and phase by EBSD was not possible in this grain as its highly polished surface did not diffract.

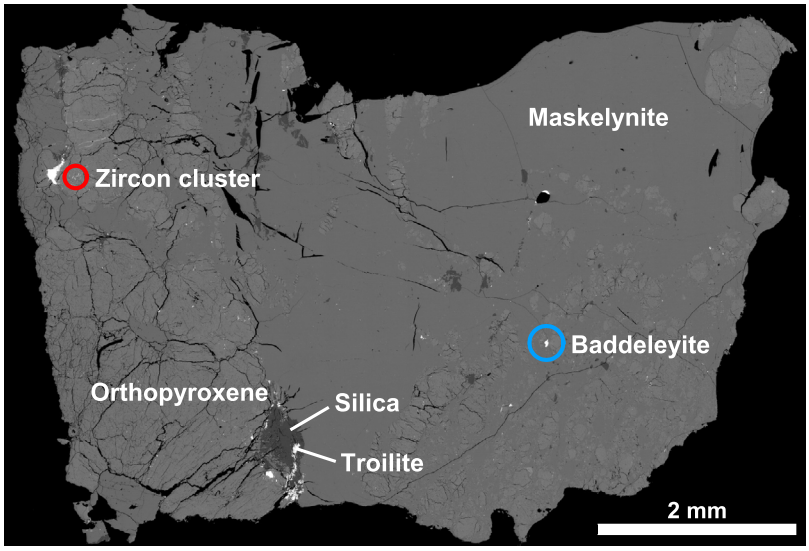

Fig. 4. Backscattered electron (BSE) mapping of thin section 78238,14. The yellow circles indicate the areas of the zircon and baddeleyite grains. The dark grey smooth phase is maskelynite, and the light grey coarse phase is orthopyroxene.

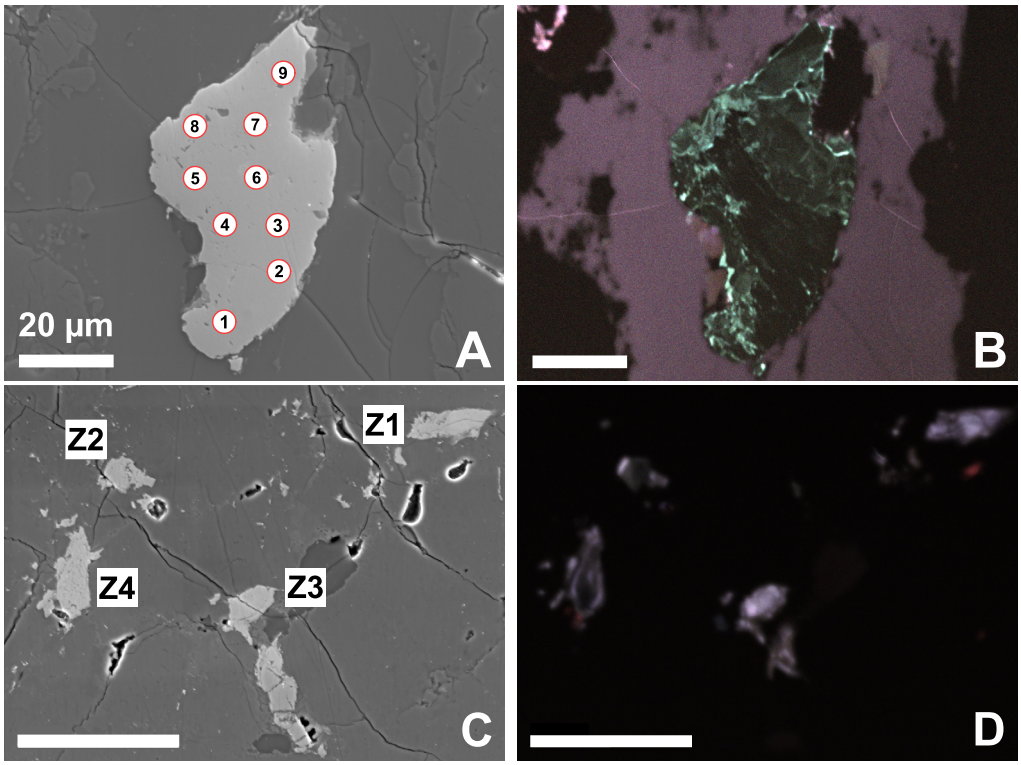

Fig. 5. Secondary electron (SE) (A and C) and CL (B and D) images of the 78238 baddeleyite (A and B) and zircon (C and D) grains. The circles indicate the location of the NanoSIMS pits.

Table 1
NanoSIMS U-Pb data and U, Th, Y trace element concentrations of zircon and baddeleyite grains in Apollo 78238,14.

Sample	Corrected $^{207}Pb/^{206}Pb$	Err Mean (1σ %)	$^{204}Pb/^{206}Pb$	$^{206}Pb/^{238}U$	Err Mean (1σ %)	U (ppm)	Y (ppm)	Th (ppm)	Th/U	$^{207}Pb/^{206}Pb$ age (Ma)	$\pm$ 1σ	$^{206}Pb/^{238}U$ age (Ma)	$\pm$ 1σ
78238,14 (individual zircons)													
Z1	0.48871	4.29	0.000797	1.0410	5.71	38	235	229	6.01	4208	62	4599	190
Z2	0.49719	5.18	0.000508	0.8672	14.9	201	719	179	0.89	4233	74	4026	463
Z3	0.52480	2.06	0.001111	1.0823	3.10	36	613	225	6.26	4312	30	4728	105
Z4	0.52533	3.81	0.000089	1.4589	3.76	191	315	267	1.40	4314	55	5800	146
78238,14 (single baddeleyite)													
B959-1	0.52452	1.33	<d.l.	0.5790	8.36	246	370	71	0.29	4312	19	2945	201
B959-2	0.53365	1.22	0.000138	0.6162	8.43	241	353	75	0.31	4337	18	3095	211
B959-3	0.52341	0.74	0.000093	0.5631	8.38	245	330	80	0.33	4309	11	2880	198
B959-4	0.53238	0.96	<d.l.	0.6295	8.36	247	335	82	0.33	4334	14	3148	212
B959-5	0.53056	1.71	0.000027	0.3121	9.48	265	327	76	0.29	4329	25	1751	147
B959-6	0.52123	1.27	0.000132	0.5608	8.55	172	263	56	0.32	4302	19	2870	201
B959-7	0.51126	0.89	0.000193	0.6942	8.81	168	208	70	0.42	4274	13	3399	237
B959-8	0.49666	1.90	0.000058	0.3642	8.59	267	368	70	0.26	4231	28	2002	150
B959-9	0.52981	1.37	0.000061	0.6340	8.40	143	171	75	0.53	4326	20	3166	214

<d.l.: below detection limit of ^{204}Pb.

3.2. U-Pb geochronology

The U-Pb data of four micro-zircons in the cluster and nine spots within the single baddeleyite grain were obtained by NanoSIMS (Table 1). Four zircon grains have $^{207}Pb/^{206}Pb$ ages ranging from 4208 $\pm$ 62 Ma to 4314 $\pm$ 55 Ma (1σ). Their U-Pb values show variable degrees of reverse discordance (Fig. S2), possibly due to U-Pb fractionation during the SIMS session and/or small-scale variations in Pb distribution, so the U-Pb ages of zircons are not included in calculating the crystallization age of 78238. The nine baddeleyite analyses define a discordia line extending from 84 $\pm$ 280 Ma (2σ; lower intercept) to 4322 $\pm$ 48 Ma (2σ; upper intercept) (Fig. 6A). The corresponding $^{207}Pb/^{206}Pb$ ages varying from 4231 $\pm$ 28 Ma to 4337 $\pm$ 18 Ma (1σ). The $^{207}Pb/^{206}Pb$ ages of the zircon and baddeleyite have two clusters at 4264 $\pm$ 22 Ma (N = 4) and 4319 $\pm$ 12 Ma (N = 9). Four oldest domains of the baddeleyite grain define a weighted mean $^{207}Pb/^{206}Pb$ age of 4332 $\pm$ 18 Ma (2σ; Fig. 6B). This age is consistent (within error) with the upper intercept U-Pb age of 4322 $\pm$ 48 Ma.

4. Discussion

4.1. Petrogenesis of 78238 and its U-rich accessory minerals

Regardless of the widespread crystallization ages indicated by multiple chronometers (Fig. 3), the Apollo 78238 norite had to crystallize before 4270 $\pm$ 20 Ma according to the K-Ar age of its maskelynite (section 2.1) (Nyquist et al., 1981). The norite was excavated by a major impact event at 4188 $\pm$ 26 Ma (Fernandes et al., 2013; Nyquist et al., 1981). It was then emplaced into a thick ejecta blanket and cooled slowly from >800 °C (Nyquist et al., 1981). The boulder was then excavated by a recent impact event

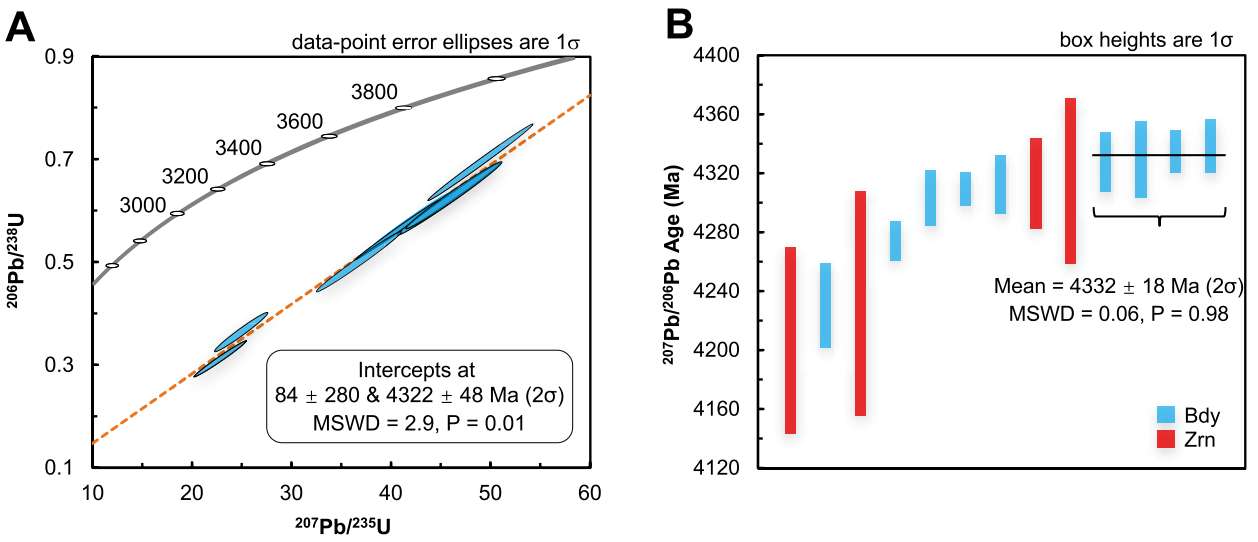

Fig. 6. U-Pb ages of zircon and baddeleyite in Apollo 78238. Panel A is the $^{206}Pb/^{238}U$–$^{207}Pb/^{235}U$ Concordia diagram for the baddeleyite grain. Panel B is the $^{207}Pb/^{206}Pb$ ages for all zircon and baddeleyite analyses. The weighted mean age of 4332 ± 18 Ma is based on the four oldest spots of the baddeleyite. Bdy = baddeleyite, and Zrn = zircon. (For interpretation of the colors in the figure, the reader is referred to the web version of this article.)

that has transported it to the recovery spot at 262 ± 5 Ma (1σ) (Fernandes et al., 2013). The U-Pb systematics of both zircon and baddeleyite are consistent with episodic loss of radiogenic Pb, presumably during a relatively recent impact event. The 262 ± 5 Ma thermochronology age is consistent with the lower intercepts of the baddeleyite U-Pb age of 84 ± 280 Ma (Fig. 6) and recent excavation of the parent boulder.

The majority of lunar zircons have features indicating primary igneous crystallization (usually with later shock alterations), while impact-grown and impact-decomposed grain textures are rare (Grange et al., 2013). No such recrystallization texture (recrystallization fronts, within-grain granulation, or interstitial growth with matrix) or decomposition signature (coexistence of silica and zirconia) is observed in our BSE and SE images of 78238,14 (Fig. 5), so these minerals are very unlikely to have recrystallized or decomposed during an impact event. The simple mineralogy and mineral pristinity of the norite support the interpretation that the U-rich minerals crystallized simultaneously with the major phases. It should be noted that we cannot rule out the possibility that the baddeleyite grain crystallized from a KREEP-rich precursor and was later incorporated into the parental magma of 78238. This scenario has recently been used to explain the presence of a baddeleyite grain in Apollo troctolite 76535, a grain that has experienced an ultra-high temperature of >2300 °C (White et al., 2020). However, xenocrystic baddeleyite is rare in the terrestrial rock cycle, and even if the 78238 baddeleyite were to be a foreign grain incorporated into the parental magma of 78238, the U-Pb systematics of the baddeleyite grain would have been disturbed or re-set during residence in dry, higher-temperature lunar magmas. As such, in either *in-situ* or "*ex-situ*" formation scenario of the 78238 baddeleyite grain, its U-Pb age represents the crystallization age of 78238. The mean (4332 ± 18 Ma) of the oldest four baddeleyite $^{207}Pb/^{206}Pb$ ages and the upper intercept (4322 ± 48 Ma) on the U-Pb Concordia diagram is consistent with the isochron ages by Sm-Nd (4334 ± 37 Ma) and Pb-Pb (4333 ± 59 Ma) (Edmunson et al., 2009) (section 3.2). We interpret the baddeleyite age of 4332 ± 18 Ma as the crystallization age of the norite. Considering the Rb-Sr (Edmunson et al., 2009) and K-Ar systems (Fernandes et al., 2013) might have been disturbed during a later impact event, the later discussion with regard to 78238 excludes the Ar-Ar and Rb-Sr ages.

4.2. Cooling rate of 78238

Borg et al. (2017) pointed out that the slow-cooling highland rocks might have significantly lower closure temperature than solidus temperature, in which case the measured radiometric ages do not record the solidification of highland rocks but merely the later closure of radiometric systems. For fast-cooling rocks, this is not an issue. For example, ferroan anorthosite 60025 has an age of 4360 ± 3 Ma (Sm-Nd and Pb-Pb mineral isochrons) estimated to have reached its solidus just a little earlier at 4383 ± 17 Ma due to its relatively fast cooling at 18 °C/Ma (Borg et al., 2017). So, the cooling rate of a highland rock is critical to interpreting its radiometric ages.

To evaluate the cooling rate of the norite boulder, we assume that the norite cooled from a solidus temperature of ~1250 °C (Borg et al., 2017). The closure temperatures (T_c) of U-Pb and Sm-Nd are evaluated using the equation from Dodson (1973), and the respective diffusion parameters are based on orthopyroxene (Nd and Pb) and zircon (Pb). The Ar-Ar and Rb-Sr ages are not included in the modeling because of the disturbance of these systems (Edmunson et al., 2009; Fernandes et al., 2013; Nyquist et al., 1981). Due to the lack of Pb diffusion data for baddeleyite, we assume the 78238 zircon grains crystallized contemporaneously with the baddeleyite grain, and the closure temperature of Pb diffusion in U-rich accessory minerals is evaluated based on the zircon grains. The diffusion parameters are derived from Cherniak (1998) for Pb and Van Orman et al. (2001) for Nd in pyroxene, and Cherniak and Watson (2001) for Pb in zircon. The diffusion radius of pyroxene grains is assumed to be 2500 μm (McCallum and Mathez, 1975), and the counterpart for zircon is 5 μm. The spherical geometric factor is 55 for all systems. The closure temperatures are calculated using incremental cooling rates ranging from 1 °C/Ma to 30 °C/Ma.

Based on the grain sizes of zircon dated in this study and pyroxene in the literature (Meyer, 2005), under different cooling rates, the closure temperatures for Sm-Nd and Pb-Pb (pyroxene), and Pb-Pb (zircon) systems vary from 973–1107 °C, 937–1055 °C, and 823–889 °C, respectively. As expected, these closure temperatures increase exponentially as the cooling rates increase (Fig. 7). The closure temperatures of Sm-Nd and Pb-Pb in 78238 are above 800 °C, so it seems that the later re-equilibration at 800 °C (McCallum and Mathez, 1975) did not induce significant disturbance

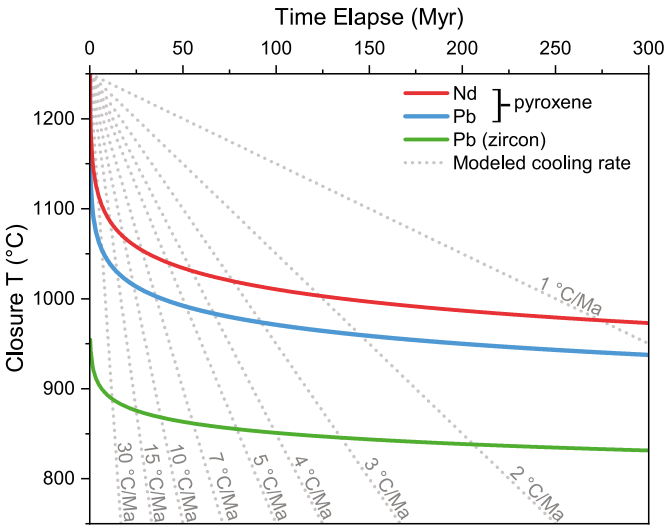

Fig. 7. Closure temperatures of Nd and Pb evaluated for the pyroxene and zircon in 78238 under different cooling rates. The closure temperatures are plotted against the time elapsed between the solidus temperature and the closure temperature. (For interpretation of the colors in the figure, the reader is referred to the web version of this article.)

on the chronometers. This partly explains why the Sm-Nd and Pb-Pb systems remained close after the primordial crystallization of 78238.

Calculating the cooling rate for 78238 is difficult with the current level of uncertainty of the overlapping Sm-Nd and Pb-Pb ages. The possibly largest age difference (including errors) between the Sm-Nd isochron age and the baddeleyite $^{207}Pb/^{206}Pb$ age is ~57 million years, which corresponds to a cooling rate of ~3 °C/Ma. This value is the lower limit (very low probability, however) for the cooling rate of 78238. In contrast, if we take at face value (i.e., excluding errors), the baddeleyite $^{207}Pb/^{206}Pb$ age together with the Sm-Nd and Pb-Pb isochron ages of 78238 support a relatively high cooling rate >30 °C/Ma (Fig. 7). The exact cooling rate of 78238 remains elusive, but the identical ages by *in-situ* dating and isochron dating support fast cooling.

Another Apollo Mg-suite rock, troctolite 76535, is thought to have a low cooling rate of 3.9 °C/Ma such that it reached solidus at 4384 ± 24 Ma while its Sm-Nd age is 4307 ± 11 Ma (Borg et al., 2017). This inferred slow cooling of 76535 in the early times is consistent with its petrographic characteristics such as very coarse grain size, homogeneous mineral compositions, 120° grain boundary junctions, and the presence of symplectites (Elardo et al., 2012; Stewart, 1975). However, 76535 could have rapid late-stage cooling, albeit slow overall cooling, based on pyroxene (McCallum et al., 2006). In the slow-cooling scenario (with a cooling rate of 3.9 °C/Ma), one would expect that $^{207}Pb/^{206}Pb$ ages of U-rich minerals in a Mg-suite rock are tens of Myr younger than its Sm-Nd mineral isochron ages (Fig. 7). As for 76535, its baddeleyite $^{207}Pb/^{206}Pb$ age (4328 ± 8 Ma) is, on the contrary, slightly older than its Sm-Nd isochron age (4307 ± 11 Ma). In this case, either 76535 is an extremely fast-cooled rock or at least one of these two crystallization ages is misinterpreted. The predominant closure ages of the primary LMO differentiates at 4.36–4.34 Ga indicate that multiple chronometers reached their closure temperatures in a short period of ~30 Myr (Borg et al., 2020). The fast-cooling scenario for 76535 and 78238 complies with the thermal state (i.e., fast cooling) on a global scale at ~4.3 Ga. Alternatively, the Mg-suite magmatism might have overlapped with FAN petrogenesis and that the cooling rates of the Mg-suite rocks might be heterogeneous within the deep crust.

4.3. Impact origin versus mantle overturn origin of the Mg-suite magmatism

The mantle overturn origin for the Mg-suite magmatism is predominantly preferred according to current modeling (e.g., Elkins-Tanton et al., 2002), petrologic studies (e.g., Prissel et al., 2016), and geochemical studies (e.g., de Vries et al., 2010). Recently, a question arises as to whether a fraction of Apollo Mg-suite rocks may possibly originate from impact melt sheets. Microstructural evidence for the impact origin of the Mg-suite has been found in Apollo troctolite 76535, which is deemed as among the most pristine Mg-suite rocks collected by the Apollo missions. Sample 76535,51 has a large, subhedral grain of monoclinic ZrO_2 (baddeleyite) with phase transformation heritage indicating a cubic precursor that was formed during an impact-induced superheated process (White et al., 2020). This grain lacks shock deformation, so it is apparently a foreign grain incorporated into the magma from which troctolite 76535 crystallized. White et al. (2020) suggested that the simplest explanation for such an admixture implies an impact melt origin for the parental magma. Thick impact melt sheets could facilitate slow cooling to form a sequence of lunar Mg-suite rocks, i.e., troctolite, norite, and gabbro (Hess, 1994). Large impacts in the initial stage of late accretion would have been capable of creating large, superheated impact melt pools that could have homogenized the target rocks. For instance, such sequential differentiated units (norite, gabbro, and granophyre) have been found in the terrestrial impact-induced Sudbury structure (Grieve et al., 1991).

Due to the vast majority of evidence supporting the mantle overturn origin of the Mg-suite parental magmas, the impact origin hypothesis faces many challenges that are best shown in Shearer et al. (2015): (1) the impact process was unable to produce either high-Mg# magmas or the inter-element (e.g., Ni and Co in olivine) trends of the Mg-suite rocks; (2) the antiquity (>4.2 Ga) of all Mg-suite rocks would require them to crystallize from the older impact melt sheets, but such structures are rare on the lunar near side, (3) the deep crustal origin of some Mg-suite rocks does not point to their crystallization from the impact melt sheets on the surface. In contrast, many other geological observations on the near side are more consistent with the mantle-overturn origin, such as the olivine and low-Ca pyroxene cumulates excavated from the upper mantle to surface (Miljković et al., 2015), the origin of high-Ti basalts from partial melting of garnet-bearing assemblages (Beard et al., 1998), and the low-viscosity zone (possibly formed by volatile-rich ilmenite-bearing cumulates penetrating the mantle) at the core-mantle boundary (Harada et al., 2016).

Impact involvement in the origin of the Mg-suite may merely be complementary to the mantle overturn origin. Firstly, an alternative explanation for the monoclinic baddeleyite in 76535 is that this grain is a pre-existing grain formed during an earlier superheated impact event and was later incorporated into the parental magma of 76535 during an assimilation process. A moderate extent of assimilation is almost inevitable in the Mg-suite context (a type of melting mainly caused by dry, adiabatic ascent from considerable depth, which implies adiabatic superheating (Warren, 1986)). Unlike most assimilated material, this unusual grain was not susceptible to dissolution when surrounded by a large mass of troctolite-parent magma. In this case, a mantle-overturn origin for the parental magma of 76535 is still valid. Even if 76535 has an impact origin, it does not falsify that the mantle overturn played a primary role in forming the Mg-suite parental magmas. We note that the crystallization ages of 76535 (4328 ± 8 Ma) and 78238 (4332 ± 18 Ma) are identical to the impact event(s) recorded in an impact-melt-grown zircon (4335 ± 5 Ma) in Apollo impact melt breccia 73217 (Grange et al., 2009) and an impact-recrystallized zircon (4332 ± 6 Ma) in Apollo breccia 15455 (Crow et al., 2016).

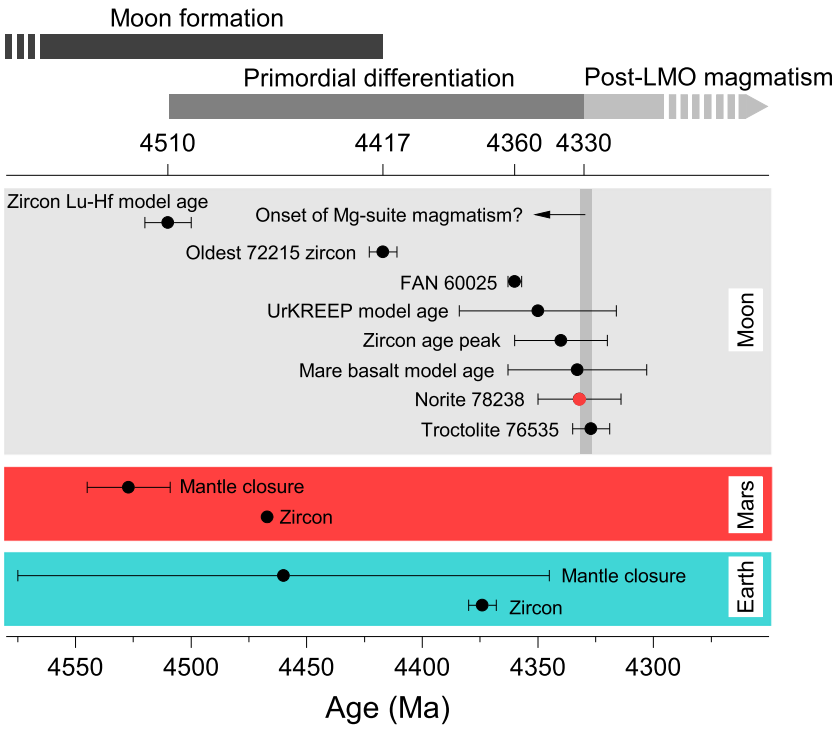

Fig. 8. Geochronological summary of the early Moon, Mars, and Earth differentiation. The chronology of lunar differentiation is defined by the Lu-Hf model age of zircon (Barboni et al., 2017), the oldest zircon U-Pb age from breccia 72215 (Nemchin et al., 2009), Pb-Pb and Sm-Nd isochron ages of FAN 60025 (Borg et al., 2011), Sm-Nd model ages of KREEP and mare basalts (Borg et al., 2020 and references therein), lunar zircon $^{207}Pb/^{206}Pb$ age peak (Borg et al., 2015 and references therein), and troctolite 76535 (White et al., 2020) and norite 78238 (this study), both by SIMS Pb-Pb dating of baddeleyite. The mantle closure (Morino et al., 2017) and oldest zircon (Wilde et al., 2001) ages of Earth, and the mantle closure (Bourdon et al., 2008) and oldest zircon (Bouvier et al., 2018) ages of Mars are shown for comparison.

It is plausible that the mantle overturn, coeval with the 4.33-Ga impact event(s), was not solely driven by unstably stratified cumulates, but rather early impact(s) facilitated the overturn process by heating and mobilizing the cumulates.

4.4. Implications for the lunar crustal formation

Norite 78238 and troctolite 76535 are among the most pristine Mg-suite members: 78238 has a pristinity index of 8/10 and 76535 of 9/10 (Shearer et al., 2015; Warren, 1993). These two critical samples are fairly representative of the Mg-suite rocks. The $^{207}Pb/^{206}Pb$ age of the baddeleyite in thin section 76535,51 at 4328 ± 8 Ma (White et al., 2020) is within error of that of 78238,14 at 4332 ± 18 Ma (Fig. 3). The baddeleyite ages for 76535 and 78238 are also within the uncertainties of the Sm-Nd isochron age of collective Apollo 14, 15, 16, and 17 Mg-suite rocks at 4348 ± 25 Ma (Borg et al., 2020). Due to the limited sampling of the Mg-suite rocks in the current collection, the 4.33 Ga ages indicated by these two samples could either mark the onset of the Mg-suite magmatism or a later pulse of the Mg-suite type of serial magmatism (Fig. 8).

Unlike the previous isochron ages (Fig. 3), the baddeleyite $^{207}Pb/^{206}Pb$ age of 78238 is younger than the age of FAN 60025 at 4360 ± 3 Ma (Borg et al., 2011). Regardless of the petrogenesis of 78235/6/8 by impact or mantle overturn processes, the $^{207}Pb/^{206}Pb$ ages of the 76535 (White et al., 2020) and 78238 U-rich minerals demonstrate that their parental magma(s) formed contemporaneously, and their formation postdates the formation of FAN 60025. The temporal relationship between the FAN and Mg-suite resolved by the SIMS Pb-Pb dating appears consistent with the LMO model (Warren, 1985).

5. Conclusions

In-situ U-Pb dating of U-rich accessory minerals zircon and baddeleyite was performed in the Apollo shocked norite 78238, an important representative of the Mg-suite rocks. We interpret the oldest $^{207}Pb/^{206}Pb$ ages of an igneous baddeleyite grain of 4332 ± 18 Ma to date the crystallization of the 78235/6/8 norite, overlapping that of Mg-suite troctolite 76535 (4328 ± 8 Ma; White et al., 2020) and distinguishably younger than the Sm-Nd and Pb-Pb isochron age of FAN 60025 (4360 ± 3 Ma; Borg et al., 2011). This result is significant because it demonstrates that the ages of the FANs and Mg-suite rocks can be resolved. It suggests that the Mg-suite is slightly (at least 10 Myr) younger than FANs, which is predicted based on the KREEP-rich nature of Mg-suite rocks (Shearer et al., 2015) and the LMO differentiation model (Warren, 1985). Such a small age difference cannot be resolved by using the Sm-Nd whole-rock isochron method for FAN and Mg-suite rocks, respectively (Borg et al., 2020). Based on the precise *in-situ* chronology of two Mg-suite rocks analyzed so far with the SIMS method, the onset of Mg-suite magmatism or at least a later pulse of the Mg-suite type of serial magmatism took place at 4.33 Ga.

The *in-situ* U-Pb dating of U-rich accessory minerals in lunar highland rocks can complement the radiometric isochron methods. When associated with microstructural analysis of U-rich accessory minerals, it can become a powerful tool to constrain the origin and timescale of the Mg-suite magmatism. So far, 76535 and 78238 are the only two Mg-suite rocks that have been dated using the SIMS U-Pb method and U-rich minerals. If such high-resolution SIMS dating of U-rich minerals is performed on numerous Apollo Mg-suite rocks, we might be able to better understand the timescale of Mg-suite magmatism and the temporal relationship within the troctolite-norite-gabbro sequence, and furthermore, how endogenic thermal processes worked together with exogenic heating (im-

pacts) to form the lunar lithological units. Thus, this study offers insights into a path forward for obtaining a precise timeline for the Mg-suite that has been limited by mineral isochron age determinations with relatively low, $\sim \pm 50$ Ma, precision.

CRediT authorship contribution statement

Bidong Zhang: Conceptualization, Formal analysis, Investigation, Methodology, Writing – original draft. **Yangting Lin:** Funding acquisition, Methodology, Writing – review & editing. **Desmond E. Moser:** Funding acquisition, Methodology, Writing – review & editing. **Paul H. Warren:** Writing – review & editing. **Jialong Hao:** Formal analysis, Investigation. **Ivan R. Barker:** Formal analysis, Investigation. **Sean R. Shieh:** Supervision, Writing – review & editing. **Audrey Bouvier:** Conceptualization, Funding acquisition, Project administration, Resources, Supervision, Writing – review & editing.

Declaration of competing interest

The authors declare that they have no known competing financial interests or personal relationships that could have appeared to influence the work reported in this paper.

Acknowledgements

We thank the Apollo 17 crew for collecting this sample and CAPTEM for allocating thin section 78238,14. We also appreciate the experimental assistance from Nian Wang and Lixin Gu (IGGCAS) in FIB-SEM. Two anonymous reviewers and Editor William McKinnon are thanked for their insightful comments to improve this work. We also acknowledge the support from the NSERC Discovery Grant (06310-2014) and Canada Research Chairs (950-229061) programs to AB, NSERC Discovery Grant (2019-05911) to DM, NSERC Discover Grant (06818-2019) to Sean Shieh, Natural Science Foundation of China (41490631) to YL, Key Research Program of Frontier Sciences, Chinese Academy of Sciences (QYZDJ-SSW-DQC001) to YL, and China Scholarship Council (201607970013) to BZ. This manuscript was prepared in part at UCLA under NASA grants 80NSSC19K1238 (BZ) and 80NSSC19K0794 (PHW).

Appendix A. Supplementary material

Supplementary material related to this article can be found online at https://doi.org/10.1016/j.epsl.2021.117046.

References

Barboni, M., Boehnke, P., Keller, B., Kohl, I.E., Schoene, B., Young, E.D., McKeegan, K.D., 2017. Early formation of the Moon 4.51 billion years ago. Sci. Adv. 3, e1602365.

Beard, B.L., Taylor, L.A., Scherer, E.E., Johnson, C.M., Snyder, G.A., 1998. The source region and melting mineralogy of high-titanium and low-titanium lunar basalts deduced from Lu-Hf isotope data. Geochim. Cosmochim. Acta 62, 525–544.

Borg, L.E., Cassata, W.S., Wimpenny, J., Gaffney, A.M., Shearer, C.K., 2020. The formation and evolution of the Moon's crust inferred from the Sm-Nd isotopic systematics of highlands rocks. Geochim. Cosmochim. Acta 290, 312–332.

Borg, L.E., Connelly, J.N., Boyet, M., Carlson, R.W., 2011. Chronological evidence that the Moon is either young or did not have a global magma ocean. Nature 477, 70–72.

Borg, L.E., Connelly, J.N., Cassata, W.S., Gaffney, A.M., Bizzarro, M., 2017. Chronologic implications for slow cooling of troctolite 76535 and temporal relationships between the Mg-suite and the ferroan anorthosite suite. Geochim. Cosmochim. Acta 201, 377–391.

Borg, L.E., Gaffney, A.M., Shearer, C.K., 2015. A review of lunar chronology revealing a preponderance of 4.34–4.37 Ga ages. Meteorit. Planet. Sci. 50, 715–732.

Bourdon, B., Touboul, M., Caro, G., Kleine, T., 2008. Early differentiation of the Earth and the Moon. Philos. Trans. R. Soc. Lond. A, Math. Phys. Eng. Sci. 366, 4105–4128.

Bouvier, L.C., Costa, M.M., Connelly, J.N., Jensen, N.K., Wielandt, D., Storey, M., Nemchin, A.A., Whitehouse, M.J., Snape, J.F., Bellucci, J.J., 2018. Evidence for extremely rapid magma ocean crystallization and crust formation on Mars. Nature 558, 586–589.

Carlson, R., Lugmair, G.t., 1981. Time and duration of lunar highlands crust formation. Earth Planet. Sci. Lett. 52, 227–238.

Carlson, R.W., Borg, L.E., Gaffney, A.M., Boyet, M., 2014. Rb-Sr, Sm-Nd and Lu-Hf isotope systematics of the lunar Mg-suite: the age of the lunar crust and its relation to the time of Moon formation. Philos. Trans. R. Soc. Lond. A, Math. Phys. Eng. Sci. 372, 20130246.

Černok, A., White, L.F., Darling, J., Dunlop, J., Anand, M., 2019. Shock-induced microtextures in lunar apatite and merrillite. Meteorit. Planet. Sci. 54, 1262–1282.

Cherniak, D., 1998. Pb diffusion in clinopyroxene. Chem. Geol. 150, 105–117.

Cherniak, D., Watson, E., 2001. Pb diffusion in zircon. Chem. Geol. 172, 5–24.

Crow, C.A., McKeegan, K.D., Moser, D.E., 2016. Coordinated U-Pb geochronology, trace element, Ti-in-zircon thermometry and microstructural analysis of Apollo zircons. Geochim. Cosmochim. Acta 202, 264–284.

de Vries, J., van den Berg, A., van Westrenen, W., 2010. Formation and evolution of a lunar core from ilmenite-rich magma ocean cumulates. Earth Planet. Sci. Lett. 292, 139–147.

Dodson, M.H., 1973. Closure temperature in cooling geochronological and petrological systems. Contrib. Mineral. Petrol. 40, 259–274.

Edmunson, J., Borg, L.E., Nyquist, L.E., Asmerom, Y., 2009. A combined Sm–Nd, Rb–Sr, and U–Pb isotopic study of Mg-suite norite 78238: further evidence for early differentiation of the Moon. Geochim. Cosmochim. Acta 73, 514–527.

Elardo, S.M., Draper, D.S., Shearer, C.K., 2011. Lunar Magma Ocean crystallization revisited: bulk composition, early cumulate mineralogy, and the source regions of the highlands Mg-suite. Geochim. Cosmochim. Acta 75, 3024–3045.

Elardo, S.M., McCubbin, F.M., Shearer Jr., C.K., 2012. Chromite symplectites in Mg-suite troctolite 76535 as evidence for infiltration metasomatism of a lunar layered intrusion. Geochim. Cosmochim. Acta 87, 154–177.

Elkins-Tanton, L.T., Van Orman, J.A., Hager, B.H., Grove, T.L., 2002. Re-examination of the lunar magma ocean cumulate overturn hypothesis: melting or mixing is required. Earth Planet. Sci. Lett. 196, 239–249.

Fernandes, V., Fritz, J., Weiss, B., Garrick-Bethell, I., Shuster, D., 2013. The bombardment history of the Moon as recorded by ^{40}Ar-^{39}Ar chronology. Meteorit. Planet. Sci. 48, 241–269.

Grange, M., Nemchin, A., Pidgeon, R., Timms, N., Muhling, J., Kennedy, A., 2009. Thermal history recorded by the Apollo 17 impact melt breccia 73217. Geochim. Cosmochim. Acta 73, 3093–3107.

Grange, M., Pidgeon, R., Nemchin, A., Timms, N.E., Meyer, C., 2013. Interpreting U–Pb data from primary and secondary features in lunar zircon. Geochim. Cosmochim. Acta 101, 112–132.

Grieve, R.A., Stoeffler, D., Deutsch, A., 1991. The Sudbury structure: controversial or misunderstood? J. Geophys. Res. 96, 22753–22764.

Harada, Y., Goossens, S., Matsumoto, K., Yan, J., Ping, J., Noda, H., Haruyama, J., 2016. The deep lunar interior with a low-viscosity zone: revised constraints from recent geodetic parameters on the tidal response of the Moon. Icarus 276, 96–101.

Hess, P.C., 1994. Petrogenesis of lunar troctolites. J. Geophys. Res., Planets 99, 19083–19093.

Jackson, E.D., Sutton, R.L., Wilshire, H.G., 1975. Structure and petrology of a cumulus norite boulder sampled by Apollo 17 in Taurus-Littrow Valley, the Moon. Geol. Soc. Am. Bull. 86, 433–442.

Lugmair, G., Marti, K., Kurtz, J., Scheinin, N., 1976. History and genesis of lunar troctolite 76535 or: how old is old. In: Lunar and Planetary Science Conference Proceedings, pp. 2009–2033.

McCallum, I., Mathez, E., 1975. Petrology of noritic cumulates and a partial melting model for the genesis of Fra Mauro basalts. In: Lunar and Planetary Science Conference Proceedings, pp. 395–414.

McCallum, I.S., Domeneghetti, M.C., Schwartz, J.M., Mullen, E.K., Zema, M., Cámara, F., Ganguly, J., 2006. Cooling history of lunar Mg-suite gabbronorite 76255, troctolite 76535 and stillwater pyroxenite SC-936: the record in exsolution and ordering in pyroxenes. Geochim. Cosmochim. Acta 70, 6068–6078.

Meyer, C., 2005. Lunar sample compendium.

Miljković, K., Wieczorek, M.A., Collins, G.S., Solomon, S.C., Smith, D.E., Zuber, M.T., 2015. Excavation of the lunar mantle by basin-forming impact events on the Moon. Earth Planet. Sci. Lett. 409, 243–251.

Morino, P., Caro, G., Reisberg, L., Schumacher, A., 2017. Chemical stratification in the post-magma ocean Earth inferred from coupled ^{146,147}Sm–^{142,143}Nd systematics in ultramafic rocks of the Saglek block (3.25–3.9 Ga; northern Labrador, Canada). Earth Planet. Sci. Lett. 463, 136–150.

Nemchin, A., Pidgeon, R., Whitehouse, M., Vaughan, J.P., Meyer, C., 2008. SIMS U–Pb study of zircon from Apollo 14 and 17 breccias: implications for the evolution of lunar KREEP. Geochim. Cosmochim. Acta 72, 668–689.

Nemchin, A., Timms, N., Pidgeon, R., Geisler, T., Reddy, S., Meyer, C., 2009. Timing of crystallization of the lunar magma ocean constrained by the oldest zircon. Nat. Geosci. 2, 133–136.

Nyquist, L., Reimold, W., Bogard, D., Wooden, J., Bansal, B., Wiesmann, H., Shih, C.-Y., 1981. A comparative Rb-Sr, Sm-Nd, and K-Ar study of shocked norite 78236-evidence of slow cooling in the lunar crust. In: Lunar and Planetary Science Conference Proceedings, pp. 67–97.

Nyquist, L., Shih, C., Reese, Y., 2008. Sm-Nd for norite 78236 and eucrite Y980318/433: implications for planetary and solar system processes. In: Lunar and Planetary Science Conference XXXIX, pp. 1437–1438.
Premo, W., Tatsumoto, M., 1991. U-Th-Pb isotopic systematics of lunar norite 78235. In: Lunar and Planetary Science Conference Proceedings, pp. 89–100.
Premo, W.R., Tatsumoto, M., 1992. U-Th-Pb, Rb-Sr, and Sm-Nd isotopic systematics of lunar troctolitic cumulate 76535-implications on the age and origin of this early lunar, deep-seated cumulate. In: Lunar and Planetary Science Conference Proceedings, pp. 381–397.
Prissel, T.C., Parman, S.W., Head, J.W., 2016. Formation of the lunar highlands Mg-suite as told by spinel. Am. Mineral. 101, 1624–1635.
Schmitt, H., Petro, N., Wells, R., Robinson, M., Weiss, B., Mercer, C., 2017. Revisiting the field geology of Taurus–Littrow. Icarus 298, 2–33.
Shearer, C.K., Elardo, S.M., Petro, N.E., Borg, L.E., McCubbin, F.M., 2015. Origin of the lunar highlands Mg-suite: an integrated petrology, geochemistry, chronology, and remote sensing perspective. Am. Mineral. 100, 294–325.
Sprung, P., Kleine, T., Scherer, E.E., 2013. Isotopic evidence for chondritic Lu/Hf and Sm/Nd of the Moon. Earth Planet. Sci. Lett. 380, 77–87.
Stacey, J., Kramers, J., 1975. Approximation of terrestrial lead isotope evolution by a two-stage model. Earth Planet. Sci. Lett. 26, 207–221.
Stewart, D.B., 1975. Apollonian metamorphic rocks – the products of prolonged subsolidus equilibration. In: Abstracts of the 6th Lunar and Planetary Science Conference, pp. 774–776.
Takeda, H., Mori, H., Miyamoto, M., 1982. Comparison of thermal history of orthopyroxenes between lunar norites 78236, 72255, and diogenites. J. Geophys. Res., Solid Earth 87.
Van Orman, J.A., Grove, T.L., Shimizu, N., 2001. Rare earth element diffusion in diopside: influence of temperature, pressure, and ionic radius, and an elastic model for diffusion in silicates. Contrib. Mineral. Petrol. 141, 687–703.
Warren, P.H., 1985. The magma ocean concept and lunar evolution. Annu. Rev. Earth Planet. Sci. 13, 201–240.
Warren, P.H., 1986. Anorthosite assimilation and the origin of the Mg/Fe-related bimodality of pristine moon rocks: support for the magmasphere hypothesis. J. Geophys. Res., Solid Earth 91, 331–343.
Warren, P.H., 1993. A concise compilation of petrologic information on possibly pristine nonmare Moon rocks. Am. Mineral. 78, 360–376.
Warren, P.H., Wasson, J.T., 1979. The origin of KREEP. Rev. Geophys. 17, 73–88.
White, L.F., Černok, A., Darling, J., Whitehouse, M.J., Joy, K., Cayron, C., Dunlop, J.N., Tait, K., Anand, M., 2020. Evidence of extensive lunar crust formation in impact melt sheets 4330 Myr ago. Nat. Astron., 1–5.
Wilde, S.A., Valley, J.W., Peck, W.H., Graham, C.M., 2001. Evidence from detrital zircons for the existence of continental crust and oceans on the Earth 4.4 Gyr ago. Nature 409, 175–178.
Wolfe, R., 1974. Interdisciplinary Studies of Samples from Boulder 1, Station 2, Apollo 17, vol. 1.
Yang, W., Lin, Y.-T., Zhang, J.-C., Hao, J.-L., Shen, W.-J., Hu, S., 2012. Precise micrometre-sized Pb-Pb and U-Pb dating with NanoSIMS. J. Anal. At. Spectrom. 27, 479–487.
Zhang, B., Lin, Y., Moser, D.E., Hao, J., Shieh, S.R., Bouvier, A., 2019. Imbrium age for zircons in Apollo 17 South massif impact melt breccia 73155. J. Geophys. Res., Planets 124, 3205–3218.
Zhang, B., Lin, Y., Moser, D.E., Hao, J., Liu, Y., Zhang, J., Barker, I.R., Li, Q., Shieh, S.R., Bouvier, A., 2021. Radiogenic Pb mobilization induced by shock metamorphism of zircons in the Apollo 72255 Civet Cat norite clast. Geochim. Cosmochim. Acta 302, 175–192.